npj | climate and atmospheric science

Article

Published in partnership with CECCR at King Abdulaziz University

https://doi.org/10.1038/s41612-025-01022-y

Driving factors and photochemical impacts of Cl_2 in coastal atmosphere of Southeast China

Gaojie Chen[1,2,3], Xiaolong Fan[1,2], Ziyi Lin[1,2,3], Xiaoting Ji[1,2,3], Ziying Chen[1,2,3], Lingling Xu[1,2] & Jinsheng Chen[1,2] ✉

The elevated levels of molecular chlorine (Cl_2) have been observed both during the daytime or nighttime, yet the key drivers influencing Cl_2 formation remain unclear. In this study, we observed the distinct daytime and nighttime peaks of Cl_2 in coastal atmosphere of Southeast China. Field observations combined with machine learning revealed that daytime Cl_2 generation was driven by nitrate (especially ammonium nitrate) photolysis, and aerosol iron photochemistry, while the N_2O_5 uptake on aerosols containing chloride contributed to nighttime Cl_2 formation. Around noon, alkane oxidation rates by Cl radicals generated from Cl_2 photolysis surpassed those of OH radicals, leading to a 44% increment in RO_2 radical levels and a 42% enhancement in net O_3 production rates. This study offers new insights into the production and loss processes of Cl_2 in the tropospheric atmosphere, emphasizing its significance in coastal photochemical pollution.

Chlorine radicals (Cl·) are highly reactive atmospheric oxidants that play a crucial role in the formation of ozone (O_3) and secondary organic aerosols (SOA)[1,2]. Currently, molecular chlorine (Cl_2) and nitryl chloride ($ClNO_2$) are the primary precursors of Cl·[3–5]. Previous studies identified $ClNO_2$ photolysis as the dominant source of Cl· in coastal and inland regions[4,6–10], particularly in the morning[5,6]. However, recent observations indicated substantial Cl_2 formation in polluted atmospheres[3,5,11], establishing Cl_2 as a significant daytime source of Cl·, especially in the afternoon[3,12].

Anthropogenic activities, such as wastewater treatment, coal combustion, the use of chlorine-containing disinfectants, and industrial processes, have been considered as potential sources of atmospheric Cl_2[9,13,14]. Additionally, Cl_2 can be produced through heterogeneous reactions involving $ClNO_2$, hypochlorous acid (HOCl), chlorine nitrate ($ClONO_2$), O_3, hydroxyl (OH) radicals, and titanium dioxide (TiO_2) with chloride on aerosols[12,15–17]. Cl_2 is also likely co-produced with $ClNO_2$ from the uptake of dinitrogen pentoxide (N_2O_5) on acidic aerosols containing chloride during the nighttime[18,19]. Recently, Peng et al. suggested that the photodissociation of aerosol nitrate is the dominant source of daytime Cl_2 in Hong Kong[3], while Chen et al. proposed a Cl_2 formation mechanism driven by aerosol iron photochemistry, accounting for over 90% of Cl_2 production in North China[20]. Despite these advancements, the key drivers of Cl_2 generation and loss processes remain elusive, limiting our further understanding of its production mechanisms.

In this study, intensive observations of Cl_2 and related factors were conducted in a coastal city of Southeast China during the autumn of 2022. Both daytime and nighttime peaks in Cl_2 levels were detected, suggesting strong local sources of Cl_2. We used the machine learning method combined with the observational data (including meteorological parameters, aerosol compositions, and trace gases) to identify the most important factors affecting Cl_2 production and loss. Box model simulations further demonstrated the photochemical impacts of Cl_2 photolysis. Overall, this study revealed the key factors driving Cl_2 production in urban environments of coastal area, providing a scientific foundation for future research aimed at quantifying its sources and assessing its impact on the atmospheric environment.

Results and discussion

Field measurement of Cl_2

Intensive measurements of Cl_2 and related parameters were carried out in a coastal city of Southeast China. As depicted in Fig. 1a, elevated Cl_2 levels were frequently observed, particularly in late autumn, accompanied by increased concentrations of $ClNO_2$, N_2O_5, and ionic components in $PM_{2.5}$. The maximum levels of Cl_2 at our study site reached up to 155 ppt, exceeding what had been reported in Nanjing[18], but were lower than those observed in Wangdu and Hong Kong (Table S1)[3,11]. Overall, Cl_2 concentrations exhibited a distinct monthly variation pattern, characterized by significantly lower levels in October compared to November. To

[1]Institute of Urban Environment, Chinese Academy of Sciences, Xiamen, China. [2]Fujian Key Laboratory of Atmospheric Ozone Pollution Prevention, Institute of Urban Environment, Chinese Academy of Sciences, Xiamen, China. [3]University of Chinese Academy of Sciences, Beijing, China. ✉e-mail: jschen@iue.ac.cn

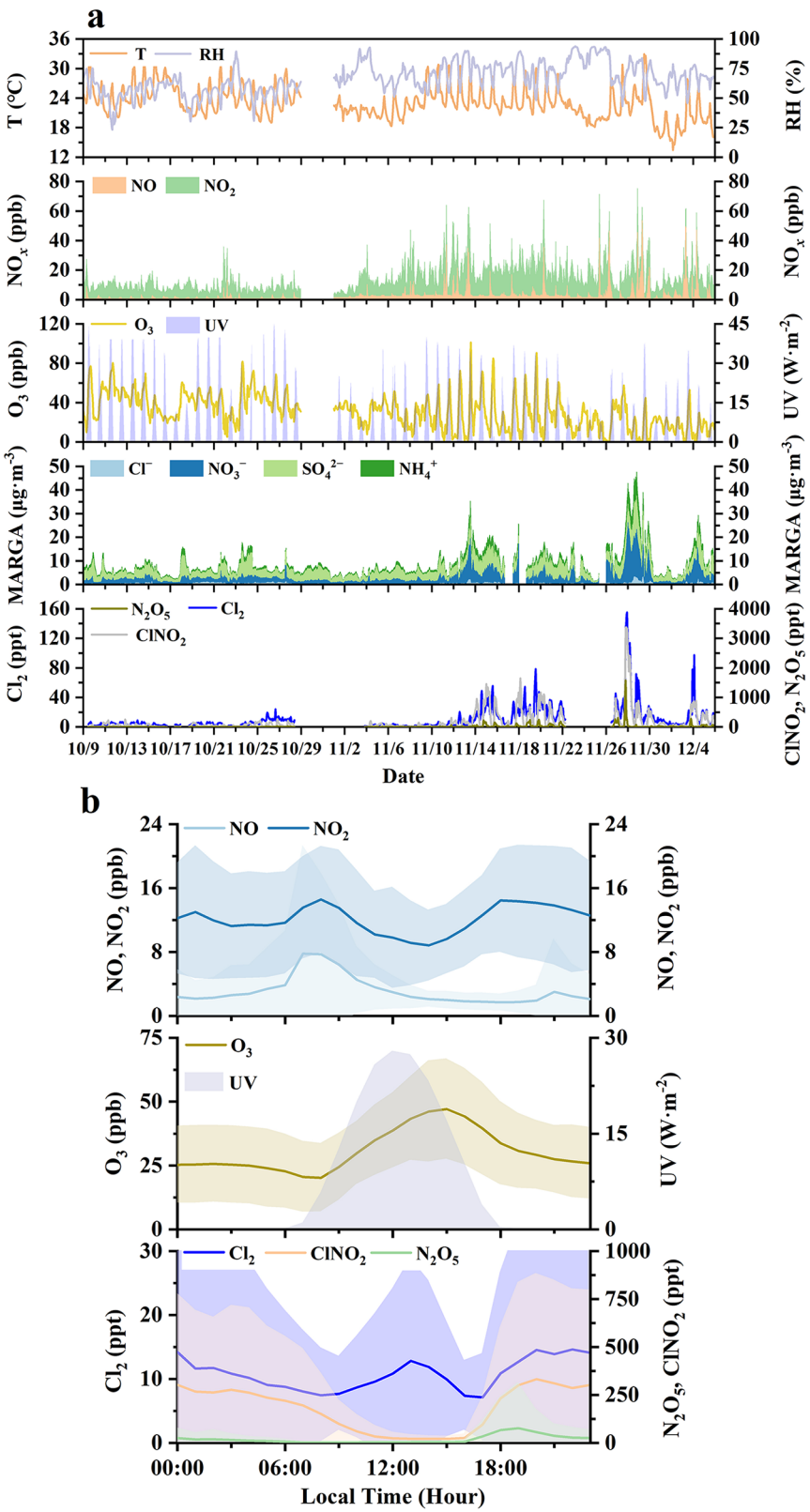

Fig. 1 | Significant generation of Cl_2 in a coastal city of Southeast China. The time series of Cl_2 and related parameters from October 9th to December 5th, 2022 (**a**). The average diurnal profile of Cl_2 and other factors during the entire observation period (**b**).

systematically investigate the influence of air mass transport on Cl_2 distribution at our study site, we conducted a comparative analysis of air mass trajectories from these two months, representing periods of lower and higher Cl_2 concentrations, respectively. Using the Hybrid Single-Particle Lagrangian Integrated Trajectory (HYSPLIT) model, we calculated 24-hour backward trajectories for air masses arriving at 500 meters above ground level[21]. The trajectory analysis demonstrated similar air mass characteristics between the two months (Fig. S1), with the study site primarily influenced by continental air masses from the northeastern coastal region, while the contribution from direct marine air masses was relatively minimal. Considering that our study site is situated in a typical urban environment, combined with the short photolytic lifetime of Cl_2, these findings strongly

suggest that Cl_2 concentration distribution is primarily driven by local generation processes, with minimal influence from regional air mass transport.

For the daily variation pattern, previous studies have reported Cl_2 peaks occurring either during the day or at night[3,11,18], but our study site showed peak concentrations during both periods (Fig. 1b), suggesting the presence of both photochemically-driven daytime sources and non-photochemical nighttime sources in the local environment.

Key influencing factors

To identify the key factors affecting the production and loss processes of Cl_2, we comprehensively compared the effects of meteorology (e.g., temperature (T), relative humidity (RH), ultraviolet radiation (UV), wind speed (WS), wind direction (WD), and boundary layer height (BLH)), $PM_{2.5}$ and aerosol compositions (e.g., iron (Fe), Cl^-, NH_4^+, SO_4^{2-}, and NO_3^-), and trace gases (e.g., N_2O_5, O_3, NO, NO_2, CO, and SO_2) on Cl_2 levels using an extreme gradient boosting (XGBoost) coupled with the Shapley additive explanations (SHAP) model (Fig. 2a). The results highlighted N_2O_5, NO_3^-, UV, NH_4^+, and Fe as the most significant factors affecting Cl_2 levels. Positive SHAP values, represented by red points, indicated that higher levels of these variables were associated with increased Cl_2 concentrations, and vice versa. As presented in Fig. 2b, larger values of N_2O_5, NO_3^-, NH_4^+, and Fe contributed to the elevation of Cl_2 levels, while UV exhibited a dual effect on Cl_2 concentrations.

Figure 2c–h further illustrates the responses of Cl_2 concentrations to changes in the five key factors, offering insights into how these factors affect Cl_2 levels on average. Cl_2 concentrations significantly increased when N_2O_5, NO_3^-, NH_4^+, and Fe concentrations exceeded 36.1 ppt, 6.2 $\mu g \cdot m^{-3}$, 3.1 $\mu g \cdot m^{-3}$, and 0.24 $\mu g \cdot m^{-3}$, respectively. Interestingly, Cl_2 levels initially decreased and then increased as rising UV intensity. After sunrise, the intensifying sunlight accelerates Cl_2 photolysis; however, under stronger UV in the afternoon, Cl_2 sources related to photochemistry might strengthen to offset its photolytic loss.

Potential production mechanisms

As mentioned before, it is found that N_2O_5, NO_3^-, UV, NH_4^+, and Fe played very critical roles in the generation of Cl_2. Here, we further explored potential Cl_2 production mechanisms associated with the five factors at our study site.

During the observation period, a strong correlation between nighttime Cl_2 and $ClNO_2$ ($r = 0.87$) was observed (Fig. 3a), implying a common source for both species during the nighttime. It is acknowledged that nighttime $ClNO_2$ is generated through the heterogeneous uptake process of N_2O_5[7,10]. Previous studies had suggested that Cl_2 is likely a byproduct of $ClNO_2$ formation through the uptake of N_2O_5 on acidic aerosols[18,19,22]. Therefore, it is probably that the heterogeneous processes involving N_2O_5 contributed to the nighttime generation of Cl_2 at our study site. The XGBoost-SHAP model indicated that N_2O_5 ranked first among all influencing factors. The positive SHAP value of N_2O_5 indicates that higher concentrations of N_2O_5 favor an increase in Cl_2 concentrations, which aligns with the mechanism that Cl_2 is primarily generated through the heterogeneous processes involving N_2O_5 during the nighttime. In contrast, the negative SHAP value of NO suggests that higher concentrations of NO inhibit the formation of NO_3, thereby hindering the increase in N_2O_5 concentrations and subsequently suppressing the generation of Cl_2.

The uptake of N_2O_5 contributed limited to daytime Cl_2 levels due to very low levels of N_2O_5 during the daytime (Fig. 1). Beyond N_2O_5, the XGBoost-SHAP model identified NO_3^- and UV as critical factors affecting Cl_2 levels. Moreover, a strong correlation ($r = 0.58$) was observed between a proxy for NO_3^- photolysis ($NO_3^- \times JNO_2 \times S_a$) and daytime Cl_2 levels during our measurement period (Fig. 3b). Recent research demonstrated that the photolysis of particulate nitrate under acidic conditions ($pH < 3.0$) is a source of daytime Cl_2, supported by both field observations and laboratory experiments[3]. We employed a thermodynamic equilibrium model (ISORROPIA II) to calculate the aerosol pH at our study site. The average aerosol pH is 2.3 ± 0.5 throughout the observation period, with the lowest values occurring during the daytime (Fig. S2). The results indicate sufficiently acidic conditions conducive to the generation of daytime Cl_2 at our study site. Therefore, it is inferred that the photolysis of particulate nitrate accounted for daytime Cl_2 formation at our study site.

Notably, previous experiment used sodium chloride (NaCl) and sodium nitrate ($NaNO_3$) as sources of particulate chloride and nitrate, with pH adjusted by sulfuric acid (H_2SO_4)[12]. However, in our study, the significance of NH_4^+ was highlighted by the XGBoost-SHAP model. Two possible explanations were explored for this. On the one hand, our analysis of chemical correlations revealed a strong positive relationship between NO_3^- and NH_4^+ ($r = 0.94$), while NO_3^- showed minimal correlation with Na^+ (Fig. S3). This correlation pattern indicates that NO_3^- formation is predominantly governed by the reaction between NH_3 and HNO_3, rather than through the acid displacement of HNO_3 on sea salt aerosols. The air mass trajectory analysis further corroborates this conclusion. Consequently, atmospheric NO_3^- at our study site exists primarily in the form of ammonium nitrate (NH_4NO_3) rather than $NaNO_3$. On the other hand, the difference in acidity between NH_4^+ and Na^+ is primarily evident in their behavior in water. Sodium salts, such as $NaNO_3$, are generally neutral since Na^+ does not react with water to change the pH. In contrast, when ammonium salts, like NH_4NO_3, dissolve, NH_4^+ reacts with water to produce ammonia and hydrogen ions, leading to an acidic solution. Consequently, ammonium salts typically decrease the value of the pH, while sodium salts do not. These results indicated that the photolysis of NH_4NO_3 mainly contribute to daytime Cl_2 generation, compared to that of $NaNO_3$. As shown in Fig. 3c, the elevated concentrations of NH_4^+ promoted the generation of daytime Cl_2 by enhancing nitrate photolysis.

In addition to the photolysis of particulate nitrate, aerosol iron photochemistry has been proposed as a major source of daytime Cl_2, accounting for over 90% of Cl_2 generation in North China[20]. In our study, Fe was identified as an important factor for Cl_2 formation based on the XGBoost-SHAP model. Furthermore, a proxy for aerosol iron photochemistry ($Fe \times JNO_2 \times S_a$) correlated well ($r = 0.61$) with daytime Cl_2 levels during our observation period (Fig. 3d). The results declared that aerosol iron photochemistry also contributed to daytime Cl_2 production at our study site.

Notably, the elevated Cl^- levels were associated with higher concentrations of Cl_2 (Fig. 2h). But once Cl^- levels exceeded 0.66 $\mu g \cdot m^{-3}$, Cl_2 concentrations tended to decline, likely due to additional limiting factors influencing Cl_2 production, implying Cl^- has not been a limiting factor at that time. Although Cl^- typically plays a significant role in the generation of Cl_2, in this study, due to the study site located in a coastal area with abundant Cl^-, the machine learning results also suggest that Cl^- is not the most critical factor influencing Cl_2 concentrations, with its importance even lower than that of SO_4^{2-}. However, this does not imply that Cl^- is not important for Cl_2 formation. Consistent with the previous observation at a coastal site of Hong Kong[3], their study also found that Cl^- is not a key limiting factor for daytime Cl_2 generation, with factors such as NO_3^- and aerosol acidity being the primary controlling variables. The importance of SO_4^{2-} likely lies in its relationship with aerosol acidity. As demonstrated in laboratory studies where acidity was regulated by H_2SO_4 to validate the process of nitrate photolysis generating Cl_2, an aerosol pH level below 3.3 is a critical condition for Cl_2 formation via nitrate photolysis[3], highlighting the significance of aerosol acidity for Cl_2 generation. Studies have shown that the high concentrations of Cl_2 observed during the daytime are closely related to aerosol acidity, while the absence of high daytime Cl_2 concentrations in many regions is primarily due to unfavorable aerosol acidity conditions for Cl_2 formation[3,23]. Therefore, the importance of SO_2 lies in its regulatory effect on aerosol acidity. Several studies have indicated that reducing SO_2 emissions can effectively modulate aerosol acidity, thereby mitigating the adverse impacts of reactive chlorine species on the atmospheric environment[3,24,25]. Meanwhile, the influence of $PM_{2.5}$ on Cl_2 is mainly determined by its chemical composition. This study found that aerosol components such as Fe, Cl^-, NH_4^+, SO_4^{2-}, and NO_3^- all contribute significantly to Cl_2 generation. The high ranking of these components in terms of factor importance may indirectly reduce the overall importance of $PM_{2.5}$, resulting in $PM_{2.5}$ having a slightly lower factor importance compared to SO_2.

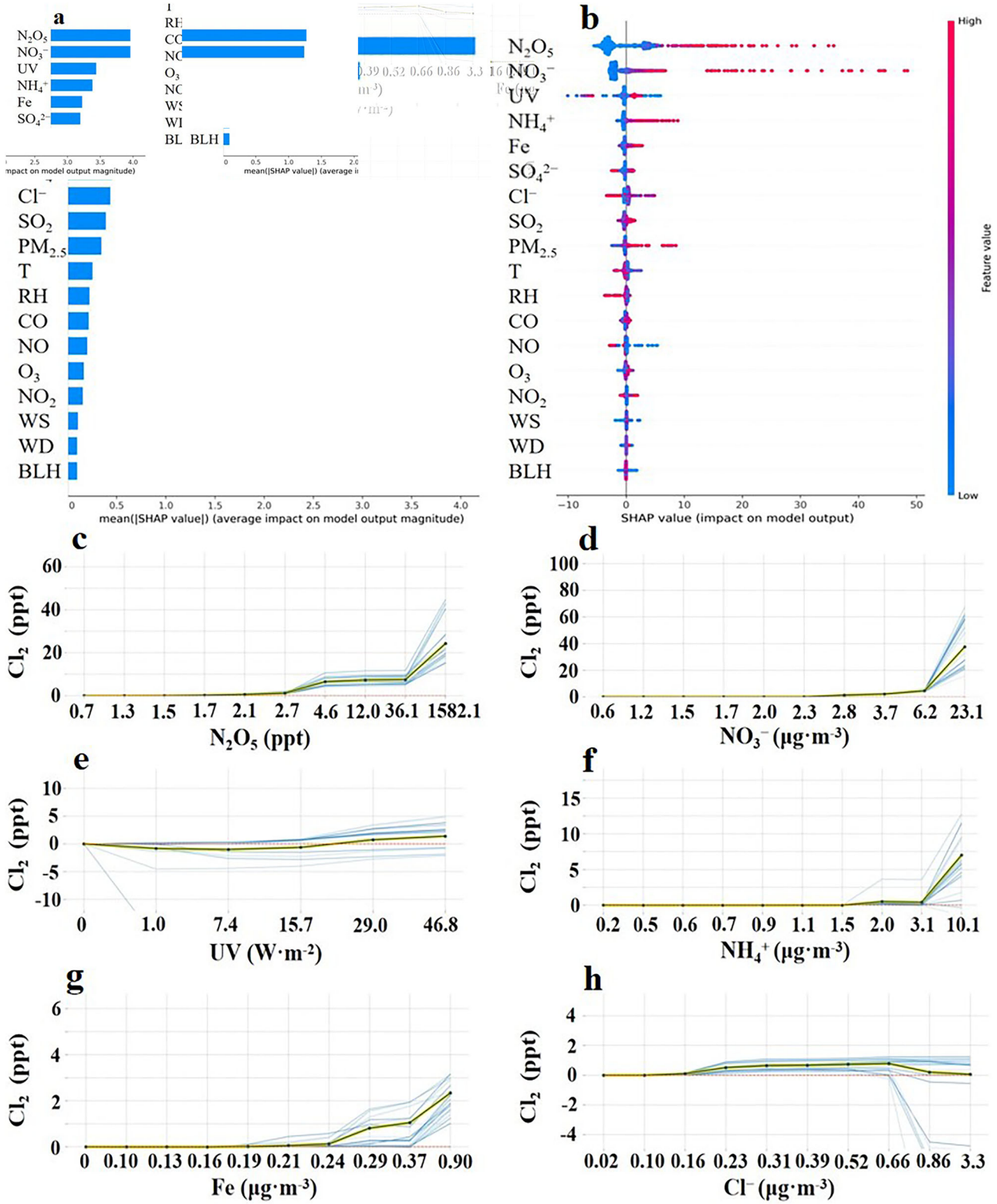

Fig. 2 | Key drivers of Cl_2 formation and loss processes. The contribution of each factor to the Cl_2 predictions (**a**). The distribution of SHAP values for all factors, ranking them by their influence on the predicted Cl_2 levels (**b**). The isolated impact of specific factors on Cl_2 levels, including N_2O_5 (**c**), NO_3^- (**d**), UV (**e**), NH_4^+ (**f**), Fe (**g**), and Cl^- (**h**). The yellow and black curves represent the average changes in simulated Cl_2 levels as the factors vary, while the blue curves illustrate all possible outcomes.

Photochemical impacts

In this study, the photochemical impacts of Cl_2 were evaluated using a box model. In contrast to the dominant role of $ClNO_2$ photolysis (up to 71%) in the early morning, Cl_2 photolysis emerged as the primary source of Cl· in the afternoon (up to 94%) (Fig. 4a). The Cl· generated from Cl_2 photolysis predominantly oxidized alkanes (~60.0%) and oxygenated volatile organic compounds (OVOCs, ~22.2%) (Fig. s4a). Meanwhile, propane, n-butane, and HCHO were the major VOC species oxidized by Cl· (Table S3). Compared to other atmospheric oxidants, such as OH·, NO_3·, and O_3, Cl· contributed to as much as 14.5% of total VOC oxidation (Fig. S4b).

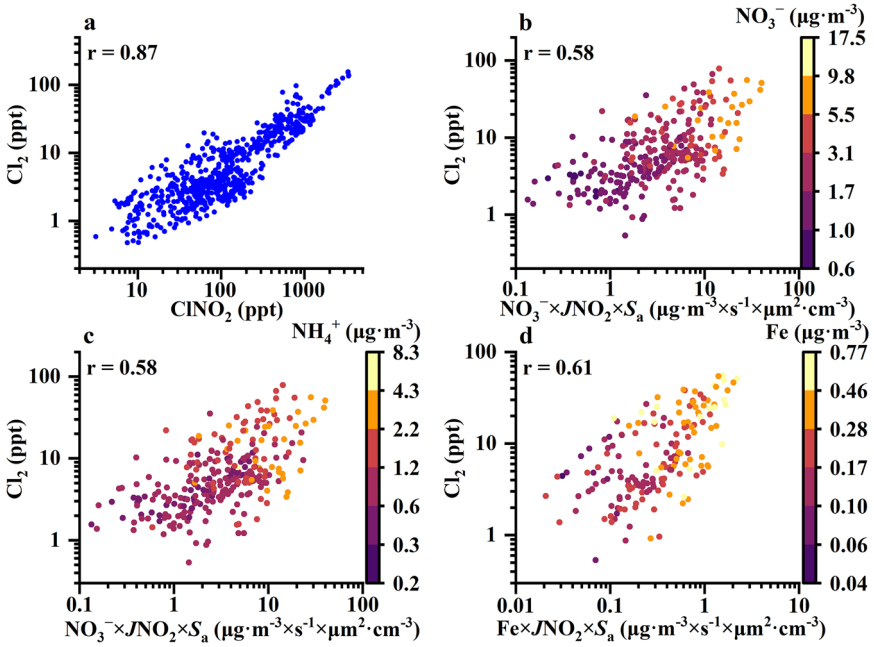

Fig. 3 | Cl_2 production mechanisms. The relationship between Cl_2 and $ClNO_2$ during the nighttime (**a**). The correlation between daytime Cl_2 concentrations (8 a.m.–4 p.m.) and a proxy of nitrate (NO_3^-) photolysis ($NO_3^- \times JNO_2 \times S_a$), and the color of the dots denotes the concentrations of NO_3^- (**b**) and NH_4^+ (**c**), respectively. The correlation between daytime Cl_2 concentrations (8 a.m.–4 p.m.) and a proxy of aerosol iron photochemistry (Fe × $JNO_2 \times S_a$), the color of the dots denotes the concentrations of Fe (**d**).

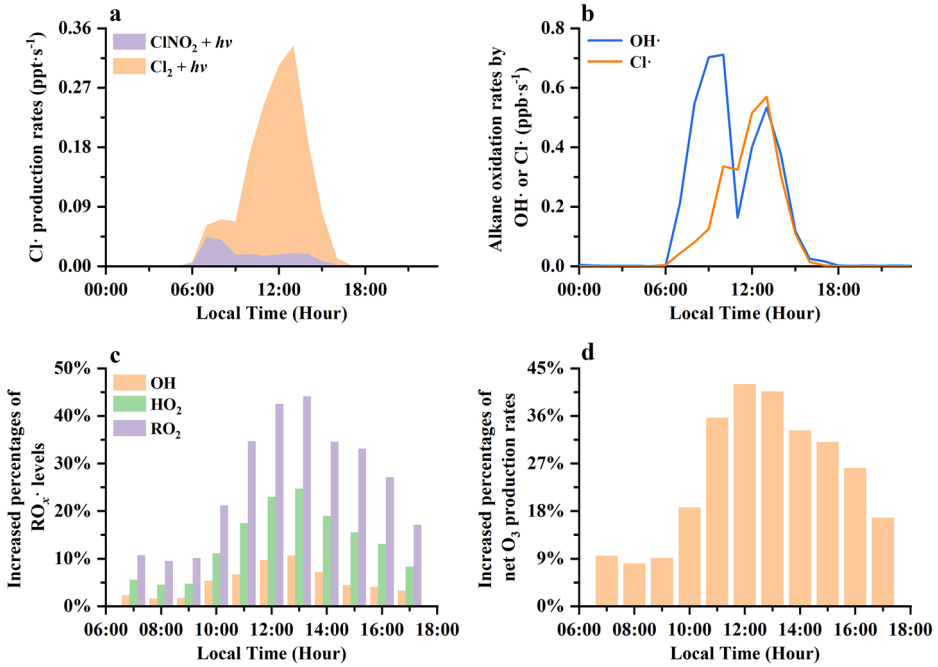

Fig. 4 | The photochemical impacts of Cl_2 on November 19th, 2022. Cl· production pathways (**a**). Comparison of alkane oxidation rates by OH· or Cl· (**b**). Increased percentages of OH·, HO_2·, and RO_2· with Cl_2 (**c**). Increased percentages of net O_3 production rates with Cl_2 (**d**).

Remarkably, around noon, alkane oxidation rates by Cl· exceeded those by OH· (Fig. S5b), mainly related to VOC, Cl·, and OH· concentrations, and their reaction rates with VOC species (Figure S5). Although the concentrations of Cl· are lower than that of OH·, the reaction rates of Cl· with alkanes are higher, particularly for ethane, propane, and n-butane (Table S4).

Cl· released from Cl_2 photolysis oxidized VOCs, facilitating the formation of RO_x (OH·, HO_2·, and RO_2·) radicals and O_3. In scenarios including Cl_2, the average concentrations of OH·, HO_2·, and RO_2· increased by 5.2%, 13.4%, and 25.9% (Fig. 4c), respectively, compared to those without Cl_2. Maximum increases in HO_2· and RO_2· levels reached 25.0% and 44.0%, greatly enhancing photochemical O_3 production through the reactions of HO_2· and RO_2· with NO. Consequently, the average net O_3 production rates increased by 42.0% in the presence of Cl_2 (Fig. 4d).

Previous studies have shown that Cl_2 concentrations typically exhibit either a single daytime peak or a nighttime peak[3,5,11,18]. However, in our study, Cl_2 concentrations displayed a dual-peak pattern during both daytime and nighttime, indicating dual sources of Cl_2 at our study site. Regarding the daytime formation mechanisms, observations from coastal areas in Hong Kong have demonstrated that the photolysis of nitrate significantly contributed to high daytime Cl_2 concentrations[3]. In contrast, observations in the inland city of Nanjing revealed a significant missing source of daytime Cl_2, which is hypothesized to be related to aerosol iron photochemistry[12], though direct observational evidence is lacking. For nighttime formation mechanisms, observations of Cl_2 in inland cities such as Nanjing and Beijing have indicated that the heterogeneous processes involving N_2O_5 are the primary source of nighttime Cl_2[5,18]. Therefore, this

study conducted systematic observations of Cl_2 in the coastal urban atmosphere of Southeast China, combined with machine learning analysis, not only revealed that both nitrate (particularly ammonium nitrate) photolysis and aerosol iron chemistry contribute to daytime Cl_2 formation but also confirmed that the heterogeneous processes of N_2O_5 dominate nighttime Cl_2 generation. Additionally, we uncovered the significant role of NH_4^+ in Cl_2 formation, an aspect that had not been clarified in previous studies. The Cl radicals released from the photolysis of high daytime Cl_2 concentrations significantly oxidized alkanes, even surpassing the alkane oxidation by OH radicals around noon. This process boosts the production of RO_x radicals and O_3, thereby altering atmospheric oxidation in urban environments of coastal area.

Methods

Field measurements

Intensive measurements were carried out at an urban site in Xiamen, a major coastal city in Southeast China, from October 9th to December 5th, 2022. The study site is situated in an urban area, characterized by proximity to river bays, shopping malls, residential zones, and major transportation routes, without the significant industrial activities in the vicinity. Further details about the site are available in our previous studies[26,27].

Cl_2, $ClNO_2$, and N_2O_5 were measured using an iodide-adduct Chemical Ionization-Atmospheric Pressure Interface-Long Time of Flight mass spectrometer (I^--ToF-CIMS, Aerodyne Research and Tofwerk AG). The concentrations of these species were calibrated following established protocols[4,13,21]. Specifically, the Cl_2 permeation tube (98 ng/min, VICI Metronics, Inc.) was used to generate standard Cl_2 gases. N_2O_5 was produced by reacting O_3 with excess NO_2, and $ClNO_2$ was synthesized through the reactions of Cl_2 with sodium nitrite ($NaNO_2$) and sodium chloride (NaCl). Additionally, the study synchronously monitored trace gases (CO, O_3, SO_2, NO_x, and volatile organic compounds (VOCs)), aerosol iron (Fe), ionic compositions in $PM_{2.5}$, aerosol surface area (S_a). Meteorological parameters were also observed, including photolysis frequencies (e.g., JNO_2), temperature (T), relative humidity (RH), ultraviolet radiation (UV), wind speed (WS), wind direction (WD), and boundary layer height (BLH)). The details on the measurement techniques and calibrations are summarized in Text S1, Text S2, and Table S1.

Machine learning model

In this study, an extreme gradient boosting (XGBoost) model was employed to predict Cl_2 levels, with the Shapley additive explanations (SHAP) model used for ranking the significance of factors influencing Cl_2 levels. The integrated XGBoost-SHAP model was utilized to identify key drivers of Cl_2 formation and loss processes. Variables included meteorological conditions (e.g., T, RH, UV, WS, WD, and BLH), $PM_{2.5}$ and aerosol compositions (e.g., Fe, Cl^-, NH_4^+, SO_4^{2-}, and NO_3^-), and trace gases (e.g., N_2O_5, O_3, NO, NO_2, CO, and SO_2). Additionally, the partial dependence plot (PDP) provided a visual representation of each factor's marginal influence on the model's predictions by systematically varying the target feature while holding other features constant. The XGBoost model exhibited strong predictive performance, with the simulated Cl_2 concentrations closely aligning with the observed concentrations ($r^2 = 0.87$, a mean absolute error of 4.2 ppt). Additional details regarding the XGBoost-SHAP model can be found in Text S3.

The box model

In our study, we utilized an observation-based model (OBM) to evaluate the photochemical effects of Cl_2. Based on prior research[14,28], we employed the Master Chemical Mechanism (MCM, Version 3.3.1) and integrated the established chlorine chemistry mechanisms. Cl_2 photolysis rates (JCl_2) were determined using the Tropospheric Ultraviolet and Visible Radiation (TUV) model under clear-sky conditions, adjusted based on observed JNO_2 values. A detailed configuration of the box model can be found in our previous studies[29]. The box model was constrained with hourly inputs of Cl_2, NO, NO_2, VOCs, O_3, SO_2, CO, along with meteorological factors. It then outputs VOC oxidation rates, RO_x (OH·, HO_2·, and RO_2·) radical levels, and O_3 production and loss rates (Text S4), comparing scenarios with and without Cl_2.

ISORROPIA II model

The aerosol pH was calculated using Eq. 1, based on the thermodynamic equilibrium model, ISORROPIA II:

$$pH = -\log_{10}\frac{1000 * H^+}{ALWC} \quad (1)$$

Here, H^+ represents the hydronium ion concentration per volume of air ($\mu g \cdot m^{-3}$), and ALWC is the aerosol liquid water content ($\mu g \cdot m^{-3}$). Inorganic particle compositions in $PM_{2.5}$ and related gases were obtained using the Monitor for AeRosols and Gases in Ambient Air (MARGA). The model was constrained by the NH_4^+-NO_3^--Cl^--SO_4^{2-}-Na^+-K^+-NH_3-HNO_3-HCl system, along with T and RH. The model setup followed protocols from previous studies[11]. Specifically, the model was run in "forward" mode, with total concentrations (gas + particle) of selected species used as inputs. Particles were considered "metastable", meaning salts did not precipitate under supersaturated conditions.

Data availability

No datasets were generated or analysed during the current study.

Code availability

The codes in this study are available from the corresponding author on reasonable request.

Received: 23 October 2024; Accepted: 25 March 2025;
Published online: 02 April 2025

References

1. Li, Q. et al. Potential effect of halogens on atmospheric oxidation and air quality in China. *J. Geophys. Res. Atmos.* **125**, e2019JD032058 (2020).
2. Li, Q. et al. Halogens enhance haze pollution in China. *Environ. Sci. Technol.* **55**, 13625–13637 (2021).
3. Peng, X. et al. Photodissociation of particulate nitrate as a source of daytime tropospheric Cl_2. *Nat. Commun.* **13**, 1–10, (2022).
4. Wang, T. et al. Observations of nitryl chloride and modeling its source and effect on ozone in the planetary boundary layer of southern China. *J. Geophys. Res. Atmos.* **121**, 2476–2489 (2016).
5. Ma, W. et al. Reactive chlorine species advancing the atmospheric oxidation capacities of inland urban environments. *Environ. Sci. Technol.* **57**, 14638–14647 (2023).
6. Phillips, G. J. et al. Significant concentrations of nitryl chloride observed in rural continental Europe associated with the influence of sea salt chloride and anthropogenic emissions. *Geophys. Res. Lett.* **39**, L10811 (2012).
7. Thornton, J. A. et al. A large atomic chlorine source inferred from mid-continental reactive nitrogen chemistry. *Nature.* **464**, 271–274 (2010).
8. Riedel, T. P. et al. Nitryl chloride and molecular chlorine in the coastal marine boundary layer. *Environ. Sci. Technol.* **46**, 10463–10470 (2012).
9. Riedel, T. P. et al. Chlorine activation within urban or power plant plumes: vertically resolved $ClNO_2$ and Cl_2 measurements from a tall tower in a polluted continental setting. *J. Geophys. Res. Atmos.* **118**, 8702–8715 (2013).
10. Osthoff, H. D. et al. High levels of nitryl chloride in the polluted subtropical marine boundary layer. *Nat. Geosci.* **1**, 324–328 (2008).
11. Liu, X. et al. High levels of daytime molecular chlorine and nitryl chloride at a rural site on the North China Plain. *Environ. Sci. Technol.* **51**, 9588–9595 (2017).
12. Chen, Q. et al. Large daytime molecular chlorine missing source at a suburban site in East China. *J. Geophys. Res. Atmos.* **127**, e2021JD035796 (2022).

13. Mattila, J. M. et al. Multiphase chemistry controls inorganic chlorinated and nitrogenated compounds in indoor air during bleach cleaning. *Environ. Sci. Technol.* **54**, 1730–1739 (2020).
14. Peng, X. et al. An unexpected large continental source of reactive bromine and chlorine with significant impact on wintertime air quality. *Natl. Sci. Rev.* **8**, nwaa304 (2021).
15. Oum, K. W., Lakin, M., DeHaan, D. O., Brauers, T. & Finlayson-Pitts, B. J. J. S. Formation of molecular chlorine from the photolysis of ozone and aqueous sea-salt particles. *Science.* **279**, 74–76 (1998).
16. Simpson, W. R., Brown, S. S., Saiz-Lopez, A., Thornton, J. A. & von Glasow, R. Tropospheric halogen chemistry: sources, cycling, and impacts. *Chem. Rev.* **115**, 4035–4062 (2015).
17. Li, Y. et al. Photoinduced production of chlorine molecules from titanium dioxide surfaces containing chloride. *Environ. Sci. Technol. Lett.* **7**, 70–75 (2020).
18. Xia, M. et al. Significant production of $ClNO_2$ and possible source of Cl_2 from N_2O_5 uptake at a suburban site in eastern China. *Atmos. Chem. Phys.* **20**, 6147–6158 (2020).
19. Yan, C. et al. Increasing contribution of nighttime nitrogen chemistry to wintertime haze formation in Beijing observed during COVID-19 lockdowns. *Nat. Geosci.* **16**, 975–981 (2023).
20. Chen, Q. et al. Impact of molecular chlorine production from aerosol iron photochemistry on atmospheric oxidative capacity in North China. *Environ. Sci. Technol.* **58**, 12585–12597 (2024).
21. Wang, H. et al. Formation and impacts of nitryl chloride in Pearl River Delta. *Atmos. Chem. Phys.* **22**, 14837–14858 (2022).
22. Roberts, J. M., Osthoff, H. D., Brown, S. S. & Ravishankara, A. R. N_2O_5 oxidizes chloride to Cl_2 in acidic atmospheric aerosol. *Scicence.* **321**, 1059 (2008).
23. Chen, G. et al. Increasing contribution of chlorine chemistry to wintertime ozone formation promoted by enhanced nitrogen chemistry. *Environ. Sci. Technol.* **58**, 22714–22721 (2024).
24. Xia, M. et al. Pollution-derived Br_2 boosts oxidation power of the coastal atmosphere. *Environ. Sci.Technol.* **56**, 12055–12065 (2022).
25. Dai, J. et al. Significant impact of a daytime halogen oxidant on coastal air quality. *Environ. Sci. Technol.* **59**, 2169–2180 (2025).
26. Hu, B. et al. Exploration of the atmospheric chemistry of nitrous acid in a coastal city of southeastern China: results from measurements across four seasons. *Atmos. Chem. Phys.* **22**, 371–393 (2022).
27. Liu, T. et al. Seasonal characteristics of atmospheric peroxyacetyl nitrate (PAN) in a coastal city of Southeast China: explanatory factors and photochemical effects. *Atmos. Chem. Phys.* **22**, 4339–4353 (2022).
28. Xue, L. K. et al. Development of a chlorine chemistry module for the master chemical mechanism. *Geosci. Model Dev.* **8**, 3151–3162 (2015).
29. Liu, T. et al. Atmospheric oxidation capacity and ozone pollution mechanism in a coastal city of southeastern China: analysis of a typical photochemical episode by an observation-based model. *Atmos. Chem. Phys.* **22**, 2173–2190 (2022).

Acknowledgements

This work was funded by the National Natural Science Foundation of China (U22A20578), the guiding project of seizing the commanding heights of "self-purifying city" (NO. IUE-CERAE-202402), the Science and Technology Department of Fujian Province (2022L3025), the National Key Research and Development Program (2022YFC3700304), STS Plan Supporting Project of the Chinese Academy of Sciences in Fujian Province (2023T3013), and Xiamen Atmospheric Environment Observation and Research Station of Fujian Province.

Author contributions

G.C. and J.C. designed the research together. G.C. analyzed data and wrote the manuscript. J.C. provided support for the research and revised the manuscript. X.F. help to perform the observation. X.F., Z.L., X.J., Z.C., and L.X. contributed to the discussion of research.

Competing interests

The authors declare no competing interests.

Additional information

Supplementary information The online version contains supplementary material available at https://doi.org/10.1038/s41612-025-01022-y.

Correspondence and requests for materials should be addressed to Jinsheng Chen.